High-Bandwidth Impedance Measurement of DC Grids Using Dual-Active Bridge Converters

Tim Karsten, Julius Kleutgens and Rik W. De Doncker
Institute for Power Generation and Storage Systems
RWTH Aachen University, Aachen, Germany
post_pgs@eonerc.rwth-aachen.de

***Abstract*—High-bandwidth impedance measurements of converters and dc grids are required for stability assessments using impedance based methods such as the passivity criterion. Furthermore, they allow conclusions about the current state of a dc grid. The measurement of converter and dc bus impedances can be conducted by disturbance injection through a converter acting on the dc bus. Literature demonstrates these methods for basic, non-galvanically isolated topologies and with limited injection bandwidth due to bandwidth limitations caused by converter control or settling behavior. This paper proposes and implements a high-bandwidth disturbance injection and impedance measurement using three-phase dual-active bridge converters. The resulting perturbation spectrum is analyzed and the effects of the injecting converter's dc link capacitance on the perturbation are investigated. An experimental verification of the method is conducted for input impedance measurement of another galvanically isolated converter. The measurement is compared to the simulated impedance profile of the device under test. The proposed disturbance injection method yields a well matching impedance measurement up to the injecting converter's switching frequency.**

***Index Terms*—broadband impedance measurement, dc system stability, dual-active bridge**

I. Introduction

Low voltage and medium voltage dc grids are a promising solution for the integration and interconnection of distributed and renewable energy sources as well as dc interfaced loads. Dc grids can increase flexibility and efficiency, while saving resources compared to ac grids. Exemplary applications are collector fields in wind farms, distribution systems in data centers and ships, and the grid integration of electric vehicle charging infrastructure [1]–[4]. All generation units, loads and grid interfaces in these dc grids are converter-based, in contrast to traditional ac systems. Consequently, stability analyses during system design and during operation require different approaches compared to traditional ac systems. Multi-terminal systems such as shown in Fig. 1 may consist of converters of different power ratings, switching frequencies, control bandwidths, and manufacturers. To implement and operate such systems, an impedance-based stability analysis is necessary,

This work has been funded by the European Union's Horizon Europe research and innovation programme under grant agreement no. 101136131 - SHIFT2DC. Views and opinions expressed in this document are those of the authors only and do not necessarily reflect those of the European Union or the European Climate, Infrastructure and Environment Executive Agency (CINEA). Neither the European Union nor the grating authority can be held responsible for them.

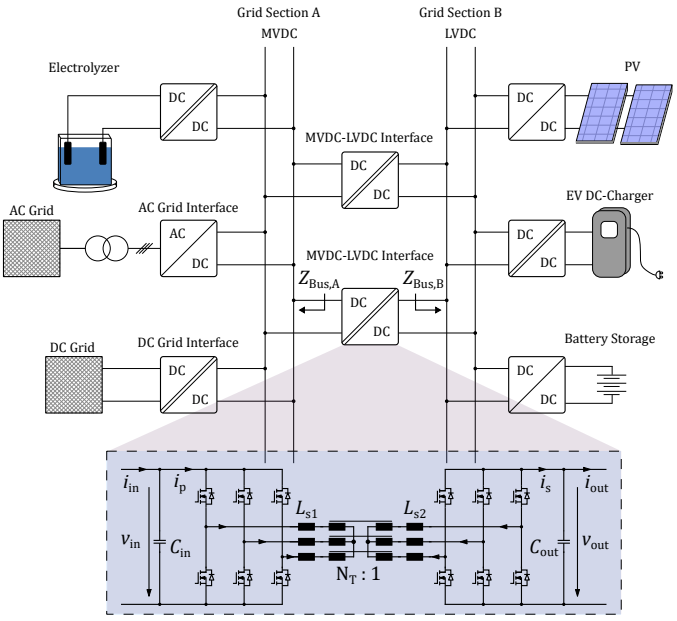

Fig. 1. Exemplary multi-converter dc system with DAB3 performing bus impedance measurement.

such as the passivity-based stability criterion, which does not rely on the knowledge of each converter's control behavior and parameters [5]. Furthermore, this approach is especially beneficial to enable multi-vendor approaches. The required impedance characteristics for each component, groups of components or the complete bus can either be attained through analytical modeling, simulation or measurement. Hence, evaluation without the requirement of knowing internal control parameters of the converters is enabled.

The impedance profile of a dc bus, a single converter, or a line can provide further insights into the current state of the system. Virtual impedances and adaptive control schemes can be implemented, using grid impedance measurements to stabilize the system [6], [7]. In case of faults, the fault location and characteristics can be determined by impedance measurement [8].

Literature proposes different methods for the online impedance measurement of converters and dc buses through disturbance injection by a converter and evaluation of the system's response [9]–[11]. However, literature mainly in-

vestigates buck and boost converters or, in the case of ac coupled systems, three-phase inverters to demonstrate the principle of impedance measurement [10]–[14]. Galvanically isolated converters are typically not considered, even though galvanic isolation or wide voltage transformation ratios are commonly required in dc grid applications. A galvanically isolated topology based on a unidirectional single-active bridge converter is employed in [15] to detect islanding operation of a pv system. The investigation is, however, limited to the use of a square wave disturbance signal and only analyzes a single frequency component in the system's response to determine passive elements connected to the system.

The dual-active bridge (DAB) is a well suited topology for dc grids, enabling high power density, galvanic isolation, bidirectional power flow, wide voltage transformation ratios, and highly dynamic control [16]–[18]. This paper proposes and demonstrates the implementation of a maximum length binary sequence (MLBS) based disturbance injection and impedance measurement using three-phase DAB (DAB3) converters. The proposed approach leverages the dynamic control capability of DABs to achieve a high bandwidth impedance measurement in the range of the DAB's own switching frequency. In systems as shown in Fig. 1, it can be assumed that only some converters might offer impedance measurement capabilities, while others may only operate in a fixed control scheme. Since the aggregated capicitance of a dc bus increases with increasing number of connected converters, a sufficiently large current perturbation is needed for a voltage response of sufficient amplitude. Consequently, higher power converters, for example converters with grid forming capabilities or converters interfacing multiple dc grid sections, may be required to inject perturbations in the bandwidth of their own switching frequency. This is necessary because converters with smaller power ratings will likely operate at higher switching frequencies and bandwidths. Furthermore, the estimation of passive components in the grid is mainly feasible at frequencies above other converters' control bandwidths.

The paper is organized as follows: section II describes the application and requirements of impedance measurements in dc grids and the employed disturbance generation and response evaluation method. The proposed impedance measurement method using a DAB3 converter is presented in section III together with considerations for practical implementations. An experimental verification and analysis is provided in section IV.

II. DC Grid Impedance Measurement

One application of dc grid impedance measurements is the assessment of dc bus stability using the passivity-based stability criterion. The passivity criterion evaluates the impedance of the one-port system attained by parallel connection of all components' impedances which are connected to the bus. The bus is considered stable if the total impedance is passive within the interaction bandwidth of the connected converters and does not have any right half plane poles [5], [19]. Up to the interaction bandwidth, the converters' control loop

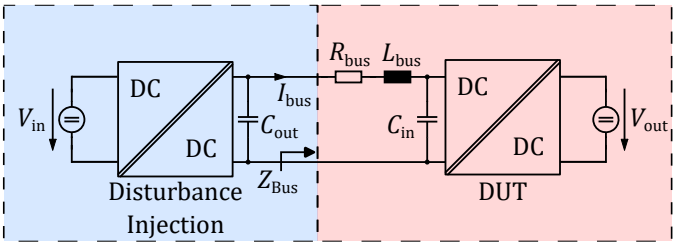

Fig. 2. Schematic of basic setup for evaluation of disturbance injection and impedance measurement of a DUT.

behavior dominates the bus' impedance behavior. At higher frequencies, the passive elements of the bus dominate the impedance profile. Therefore, impedance measurements at frequencies above the converters' interaction bandwidth may be of interest to estimate the parameters of passive elements in the dc grid. During normal operation, the estimation of passive components' values allows conclusions about the current state and configuration of the dc grid. During a fault scenario, these parameters can provide insight into the fault's location and impedance.

To reduce system complexity and cost, it is beneficial if the impedance measurement in a dc grid can be conducted by an already existing converter, instead of an additional converter which is specifically designed for impedance measurement. Consequently, the injecting converter's switching frequency may be in the same range as, or even smaller, than the switching frequency of the other converters in the system. A disturbance injection bandwidth in the range of the injecting converter's switching frequency is therefore of interest.

The concept of impedance measurement of a single converter, prior to its integration into a dc system or directly connected to another converter, is visualized in Fig. 2. The injecting converter operates in a large-signal operating point, while a small-signal disturbance is added to perturb the device under test (DUT). The generation of the disturbance signal and evaluation of the system's response are described in the following.

A. Disturbance Generation and Response Evaluation

Different types of disturbance signals have been proposed and evaluated in literature for different measurement scenarios. Under ideal conditions, sine sweeps lead to the most precise results since they only perturb one single frequency at a time [10]. However, to achieve a wide measurement bandwidth with a sufficiently high resolution, the resulting sine sweep requires a long measurement time. Additionally, the disturbance injecting device requires a sufficiently high bandwidth to generate sinusoidal outputs within the desired measurement bandwidth. In contrast, impulse based perturbations allow immediate broadband measurement, but have the drawback of a non-uniform frequency spectrum and may require a high perturbation amplitude for a sufficiently high system response amplitude [10]. For impedance measurements of converters and grids, it is beneficial to perturb the system with a periodic

broadband signal with a flat spectrum [10]. This ensures small-signal perturbation at all frequencies and enables a broadband measurement as previously described. The use of MLBS has been proposed for this purpose in literature [10]. MLBS are a type of pseudo-random signal, with properties similar to white noise. The implementation of MLBS generation is simple and can be achieved by a linear-feedback shift register. The arrangement of the shift register structure is derived based on primitive polynomials. The length L of the MLBS depends on the primitive polynomial's degree N, corresponding to the length of the shift register, according to (1). During each step of the sequence, the MLBS has one of two signal levels. After the duration T_{MLBS}, determined by the frequency f_{gen} at which the sequence is generated and its length, the MLBS repeats (cf. (2)).

$$L = 2^N - 1 \tag{1}$$

$$T_{\mathrm{MLBS}} = \frac{L}{f_{\mathrm{gen}}} \tag{2}$$

MLBS are deterministic signals and therefore enable repeatability of measurements and pre-calculation of the sequence. The frequency spectrum of a 12-bit MLBS is indicated by the red plot in Fig. 3 for a generation frequency of 20 kHz. The magnitude is constant below the generation bandwidth and drops by 3 dB at 90% of the generation frequency.

Impedance measurements can be conducted by injecting a small-signal MLBS-based current or voltage perturbation and measuring the response of the system. Fourier transformation of the measurements allows calculation of the impedance at each frequency. A transfer function can be fitted to the measured impedance points to attain a parametric transfer function, if required. Measurements of the injected disturbance and the system's response can be conducted by the injecting converter or an external measurement system. The converter's current and voltage sensors require a sufficient bandwidth and sampling rate of at least twice the highest frequency to be measured. Additionally, the control or measurement system needs to be able to sample at least the entire disturbance signal length as given by (2). Evaluation of the sampled data can either be performed by the converter's control platform or by a higher level system control unit.

The smallest measurable frequency of the impedance is determined by the length of the MLBS T_{MLBS}. The highest measurable frequency is limited by the bandwidth within which the MLBS' spectrum is considered flat, i.e. 90% of the generation frequency, assuming the voltage and current measurements have a sufficiently high sampling rate. If required, zero padding and windowing can be applied. The same MLBS perturbation can be injected multiple times, and logarithmic averaging can be applied to the measurements to decrease the effect of noise [10]. Further adjustments, depending on the application case, include approximation of blue noise to increase the high frequency content of the perturbation, the use of orthogonal signals for simultaneous injection of multiple perturbations, inverse-repeat sequences to suppress non-linearities and discrete interval sequences to concentrate the perturbation spectrum to defined frequencies [9].

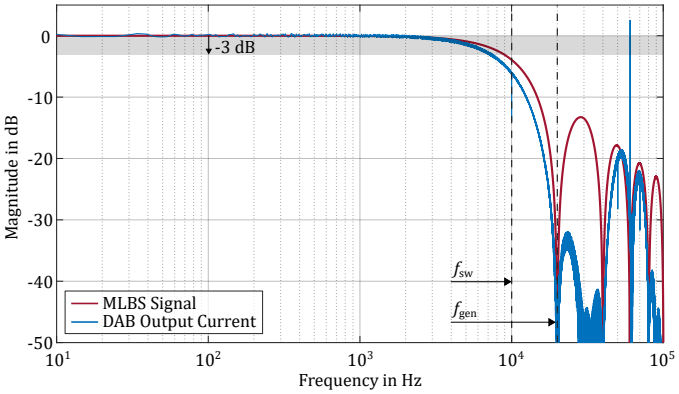

Fig. 3. Spectrum of MLBS signal and resulting DAB3 output current.

III. Disturbance Injection using Dual-Active Bridge

The practical implementation of an MLBS-based disturbance injection is presented in the following for the DAB3. Here, single phase shift (SPS) modulation is used but the method can also be extended to further modulation schemes proposed in literature, such as asymmetric duty cycle control (ADCC) [18]. Under the assumption of ideal switching behavior and a transformer magnetizing inductance much larger than the series inductance, the steady-state secondary side current I_{s} is calculated according to (3) in SPS operation [16]. Similarly, expressions for negative phase shifts and for phase shifts between $\pi/3$ and $\pi/2$ can be derived.

$$I_{\mathrm{s}} = \frac{V_{\mathrm{in}} N_{\mathrm{T}}}{2\pi f_{\mathrm{sw}} L_{\mathrm{s}}} \varphi \left(\frac{2}{3} - \frac{\varphi}{2\pi} \right), \; 0 < \varphi < \frac{\pi}{3} \tag{3}$$

The current I_{s} is the average of the instantaneous current i_{s} (cf. Fig. 1) over one sixth of a switching period. It depends only on the input voltage V_{in}, transformer series inductance L_{s} and turns ratio N_{T}, switching frequency f_{sw}, and phase shift φ between primary and secondary side. Therefore, a disturbance current can be injected into a dc bus or DUT directly by controlling the phase shift of the DAB3 accordingly. In case of a dc short circuit, the output current remains controllable by implementation of a fault-ride-through (FRT) modulation based on ADCC [18], [20]. These FRT capabilities and ADCC can extend the proposed disturbance injection scheme across the whole operating range of the DAB3, even to low-voltage or fault scenarios. To overcome bandwidth limitations of other implementations of impedance measurement proposed in literature, the application of instantaneous current control (ICC) in the DAB3 is explained in the following.

A. Control Method

From the steady-state transfer function (3), the expression for a feedforward control of the output current is derived to (4), with the transformer series reactance (5). Equation (4) is valid for reference currents $0 < I_{\mathrm{ref}} < V_{\mathrm{in}} N_{\mathrm{T}} / 12 f_{\mathrm{sw}} L_{\mathrm{s}}$. Similar

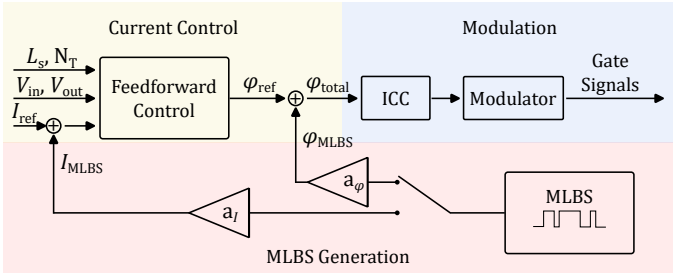

Fig. 4. Schematic of the proposed disturbance injection scheme of the DAB3.

expressions can be derived for the remaining operating range of the DAB3.

$$\varphi_{\mathrm{ref}} = \frac{2\pi}{3} - \sqrt{\frac{4\pi^2}{9} - \frac{2\pi X_{\mathrm{s}} I_{\mathrm{ref}}}{V_{\mathrm{in}} N_{\mathrm{T}}}} \tag{4}$$

$$X_{\mathrm{s}} = 2\pi f_{\mathrm{sw}} L_{\mathrm{s}} \tag{5}$$

Applying ICC to the reference phase shift φ_{ref} generated by the feedforward control allows highly dynamic changes of the DAB3's ac currents and dc currents [21]. If transients of the phase shift reference were directly applied to the DAB, the ac currents would exhibit a dc bias, and the ac and dc currents would settle depending on the time constant of the transformer's series inductance and resistance. Two ICC methods for transient changes of the phase shift are proposed in literature [21]. In this paper, the three-step method is applied because it allows instantaneous control of the current also for sign changes of the phase shift. Depending on the amplitude of the disturbance signal and the large-signal operating point of the DAB3, the phase shift can cross zero due to the disturbance injection. The current settles within half of a switching period using the three-step method, allowing an effective MLBS generation frequency of twice the DAB3's switching frequency $f_{\mathrm{gen}} = 2 \cdot f_{\mathrm{sw}}$. If the sum of the large-signal operating point of the DAB3 and the disturbance amplitude result in no transient zero crossings of the phase shift during disturbance injection, the two-step ICC method can be applied. In this case, the ac currents within the DAB3 settle within one third of the switching frequency, further increasing the potential maximum MLBS generation frequency to $f_{\mathrm{gen}} = 3 \cdot f_{\mathrm{sw}}$.

The MLBS sequence is added directly to the phase shift or to the current reference. The resulting control loop diagram is shown in Fig. 4. If the DAB3 operates in voltage or droop control, an outer control loop can be added which sets the large-signal reference current I_{ref}. In case any outer feedback control loops are added, the perturbation spectrum will be damped within their respective bandwidth. An outer control loop would react to the disturbance measured in the physical plant if the perturbation signal is added within the inner control loop only, i.e. to the phase shift or the current reference. In these cases, the MLBS signal has to be added to the reference signals of the outer control loops as well, scaled by a constant gain factor to compensate the control loops' disturbance rejection [12].

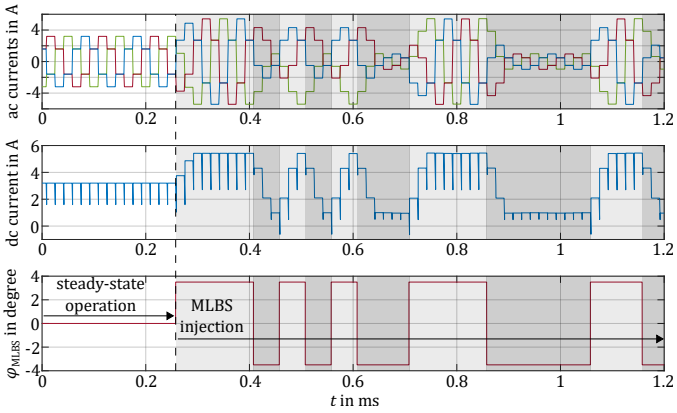

Fig. 5. Simulated ac and dc currents of the DAB3, and corresponding MLBS perturbation signal imposed on the phase shift during disturbance injection.

To achieve an effective disturbance injection frequency at twice the switching frequency, a double update of the control blocks can be used. However, due to the deterministic nature of the MBLS signal, the next two upcoming phase shift or current values can be pre-calculated during each switching period and only a single update is required. The simulated ac and dc currents of the DAB3 performing the proposed disturbance injection scheme are shown in Fig. 5 for direct injection of the MLBS into the phase shift. The desired settling time of the currents within half a switching period is observed for each step of the MLBS.

A Fourier transform of the MLBS perturbation signal and the DAB3's output current is shown in Fig. 3. Both methods, injecting the MLBS signal through the current reference or the phase shift, lead to the same result in simulation, assuming the gains a_I and a_φ for MLBS injection are chosen such that the amplitude of the resulting injected current is the same. If the series inductance value used in the feedforward control does not match the physical value, a mismatch of injected current amplitude results. However, injection through the reference current allows for a constant perturbation current amplitude if the injecting DAB3's input voltage varies. Fluctuations of the input voltage are compensated by the feedforward control according to (4). If the perturbation signal is added directly to the phase shift reference, variations of the DAB3's input voltage are not compensated and will be reflected in the output disturbance current, as described by (3).

The magnitude of the injected current drops by $3\,\mathrm{dB}$ at $7\,\mathrm{kHz}$ in Fig. 3. This decrease of effective bandwidth in which the perturbation spectrum is flat, compared to the ideal MLBS spectrum, is due to the settling time of the DAB3's currents. Even though ICC is applied, the currents do not settle instantaneously, but within half a switching period. An ideal MLBS signal assumes instantaneous transitions with infinite bandwidth while switching between its two binary states, and therefore achieves a greater perturbation bandwidth.

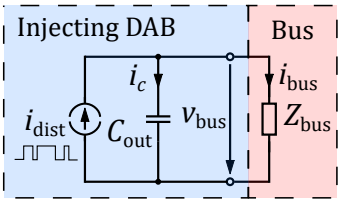

Fig. 6. Small-signal equivalent circuit of the DAB3 performing impedance measurement.

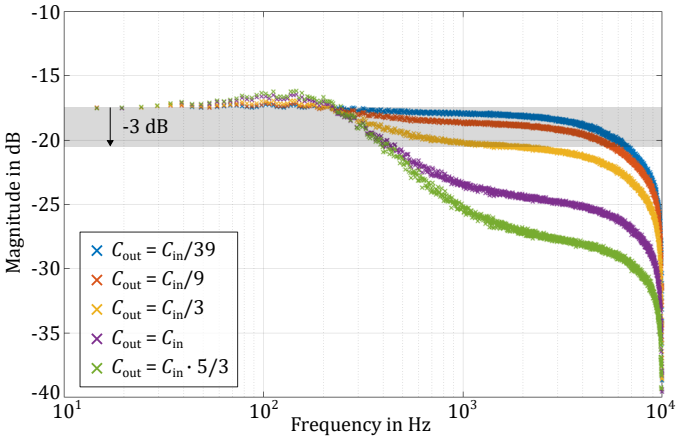

Fig. 7. Spectrum of the bus current during MLBS injection for varying ratios of the DAB3's output capacitance to DUT capacitance.

B. Influence of DC Link Capacitance

The influence of the DAB3's dc link capacitance on the bus impedance measurement is analyzed with the small signal equivalent circuit in Fig. 6. Under the proposed control scheme, the secondary side current i_{s} of the DAB3 can be modeled as a current source with the DAB3's dc link capacitor connected in parallel to the DUT. The relationship between the disturbance current i_{dist} and the bus current i_{bus} is described by the ratio of the DAB3's dc link impedance to the bus impedance according to (6).

$$i_{\text{bus}} = \frac{i_{\text{dist}}}{1 + Z_{\text{bus}}/Z_{\text{out}}} \tag{6}$$

To attain a sufficiently flat frequency spectrum of the current injected into the dc bus, the injecting converter's dc link impedance has to be greater than the bus impedance seen from the injecting converter's point of view. In case the DUT is a single converter or load, this condition is satisfied if the DUT has a sufficiently greater dc link capacitance than the injecting converter. In case of a dc bus interfacing multiple converters, it can be assumed that the aggregated bus capacitance is greater than the injecting DAB3's dc link capacitance due to the capacitive nature of voltage source converters. Significant cable lengths between converters have to be considered, as they increase the impedance seen from the injecting converter's point of view in the high frequency range.

The test setup shown in Fig. 2 was used in simulations to validate and investigate the influence of the impedance ratio

TABLE I
EVALUATION PARAMETERS

Parameter	Injecting DAB3	DUT
Input voltage V_{in}	120 V	120 V
Output voltage V_{out}	120 V	120 V
Transformer winding ratio N_{T}	1	1
Transformer series inductance L_{s}	25 µH	25 µH
Switching frequency f_{sw}	10 kHz	30 kHz
Dead time t_{dead}	300 ns	300 ns
MLBS generation frequency f_{gen}	20 kHz	
MLBS order N	12	
Bus resistance R_{bus}	100 mΩ	
Bus inductance L_{bus}	200 nH	
Bus capacitance $C_{\text{out}} + C_{\text{in}}$	244 µF	

on the injected current perturbation's frequency spectrum. The parameters listed in Table I were used for the simulations, and the ratio of the injecting DAB3's output capacitance to the DUT's input capacitance was varied. The DUT was also a DAB3, regulating the bus voltage with a PI controller. Fig. 7 shows the effect of different ratios of the DAB3's output capacitance to the bus capacitance on the perturbation spectrum. Significant damping of the MLBS magnitude occurs at frequencies above 400 Hz for capacitance ratios larger than $C_{\text{out}}/C_{\text{in}} = 1/3$. It is important to note, that the damping of the output current disturbance depends on the ratio of the output impedance to the bus impedance, not just the bus capacitance. The decrease of the perturbation current's magnitude occurs above the interaction bandwidth of the bus, where the converters' dc link capacitance starts to dominate the overall impedance. The results confirm the feasibility of the method when measuring multi-converter systems with capacitive dc links.

It is concluded that in measurement scenarios where the DAB3 is used to evaluate a single converter's impedance, it might be necessary to decrease the output capacitance of the DAB3 to optimize the resulting perturbation spectrum. In measurement scenarios of multi-converter systems, typically the bus capacitance can be assumed to be sufficiently larger than the injecting DAB3's output capacitance. Overall, the use of the three-phase DAB is especially beneficial for disturbance injection, since it inherently only requires a reduced dc link capacitance compared to its single-phase equivalent [16]. If the injecting DAB3's dc link impedance is smaller than the bus impedance and can not be further adjusted, the MLBS generation can be adapted to increase the high frequency content of the perturbation signal. This can be achieved by use of a blue-noise approximation as proposed in literature [11].

IV. EXPERIMENTAL VERIFICATION

The proposed implementation of disturbance injection and impedance measurement using a DAB3 converter is investigated with the arrangement schematically shown in Fig. 2, under the operating conditions listed in Table I. A view of

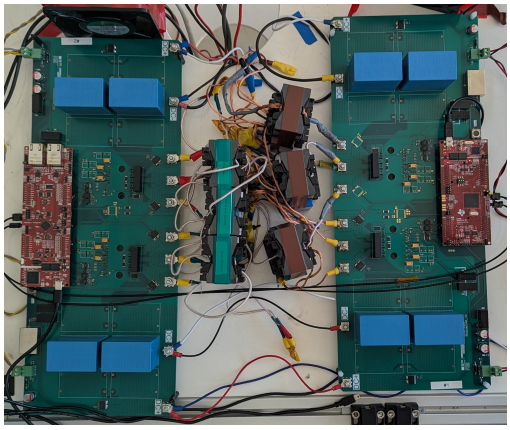

Fig. 8. View of the experimental setup, including both converters, magnetic components and control platforms.

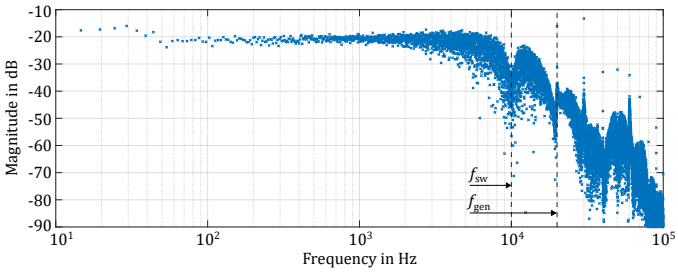

Fig. 9. Spectrum of the experimentally measured DAB3 output current under perturbation injection.

the experimental setup is given in Fig. 8. The DUT regulated its input voltage using a PI control loop and the injecting DAB3 provided a steady-state current of 3.5 A. By using the proposed disturbance injection scheme, the input impedance of the DUT was measured. The spectrum of the injected disturbance current and the measured admittance of the DUT are shown in Fig. 9 and Fig. 10. The bus current spectrum during disturbance injection is mainly flat up to 90% of the switching frequency, similar to the previously presented simulations. However, compared to the simulations, a larger spread of the magnitudes between different frequency components above 1 kHz is observed. Even though the injecting DAB3 and the DUT have the same dc link capacitance, the damping effect of the output dc link is not as pronounced as in the simulation case presented in section III. A damping of the disturbance current by 3 dB is visible, starting at frequencies above 30 Hz. The damping occurs at this frequency because the voltage control loop bandwidth of the DUT ends around 60 Hz. The dc link capacitance of the DUT starts to dominate the DUT's input impedance above 100 Hz, as observed in Fig. 10. The measured and simulated DUT admittance are shown in magnitude and phase. The simulated admittance was attained by injecting an ideal disturbance current based on the same MLBS sequence as in the experiment and using the same hardware and control parameters as in the experiment.

The measured admittance matches the simulated reference

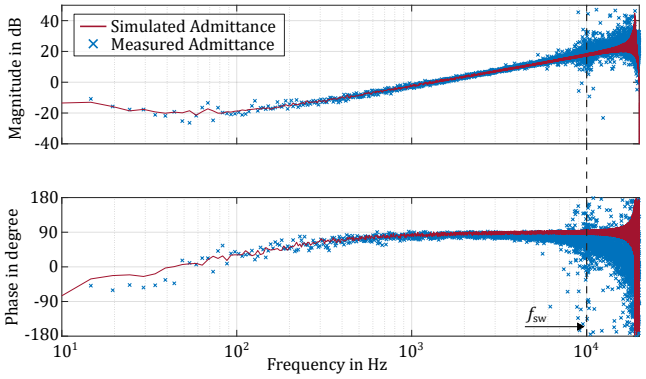

Fig. 10. Experimentally measured admittance of DUT and reference admittance attained through simulation.

of the DUT very well up to the switching frequency of the disturbance injecting DAB3. The length of the MLBS can be increased to increase the measurement resolution in the low frequency range. In the high frequency range of the measurement, magnitude and phase match the simulated values and only decrease in accuracy above the switching frequency of the injecting DAB3. Even though the spectrum of the injected current is not flat up to the switching frequency, a sufficiently accurate impedance measurement results. Deviations between simulated and measured admittance are due to modeling inaccuracies of the DUT in the simulation and effects of noise on the measurement. Additionally, the simulated DUT admittance does not consider switching noise of the injecting DAB3 or a non-ideal disturbance current spectrum.

V. Conclusions

An impedance measurement implementation for application in dc grids and evaluation of single converters has been proposed in this paper for the DAB3 converter. Employing feedforward control and ICC allows a high-bandwidth disturbance injection, as the obtained simulation results confirm. An analysis of the perturbation spectrum resulting from different output impedances of the DAB3 is provided. The presented experimental results verify the applicability of the proposed disturbance injection method for impedance measurement, and the suitability of the DAB3 for high-bandwidth impedance measurements in dc grids.

Future work will evaluate the proposed method in a larger dc system, consisting of multiple different converters. The necessity of adjusting the perturbation signal under different application scenarios will be evaluated, together with the effect of an outer voltage control loop acting on the injecting DAB3. Further improvements to the impedance measurement and calculation will be explored.

References

[1] M. Stieneker, "Analyse von Mittelspannungsgleichstromnetzen in Offshore-Windparks," Ph.D. dissertation, RWTH Aachen University, Aachen, 2017.

[2] B. R. Shrestha, U. Tamrakar, T. M. Hansen, B. P. Bhattarai, S. James, and R. Tonkoski, "Efficiency and reliability analyses of ac and 380 v dc distribution in data centers," *IEEE Access*, vol. 6, pp. 63 305–63 315, 2018.

[3] T. Ericsen, N. Hingorani, and Y. Khersonsky, "Power electronics and future marine electrical systems," *IEEE Transactions on Industry Applications*, vol. 42, no. 1, pp. 155–163, 2006.

[4] M. Stieneker, B. J. Mortimer, A. Hinz, A. Müller-Hellmann, and R. W. De Doncker, "Mvdc distribution grids for electric vehicle fast-charging infrastructure," in *2018 International Power Electronics Conference (IPEC-Niigata 2018 -ECCE Asia)*, 2018, pp. 598–606.

[5] A. Riccobono and E. Santi, "Stability analysis of an all-electric ship mvdc power distribution system using a novel passivity-based stability criterion," in *2013 IEEE Electric Ship Technologies Symposium (ESTS)*. IEEE, 2013, pp. 411–419.

[6] A. Barkley, R. Dougal, and E. Santi, "Adaptive control of power converters using digital network analyzer techniques," in *2011 Twenty-Sixth Annual IEEE Applied Power Electronics Conference and Exposition (APEC)*. IEEE, 2011, pp. 1824–1832.

[7] J. Siegers, S. Arrua, and E. Santi, "Stabilizing controller design for multibus mvdc distribution systems using a passivity-based stability criterion and positive feedforward control," *IEEE Journal of Emerging and Selected Topics in Power Electronics*, vol. 5, no. 1, pp. 14–27, 2017.

[8] E. Christopher, M. Sumner, D. W. P. Thomas, X. Wang, and F. de Wildt, "Fault location in a zonal dc marine power system using active impedance estimation," *IEEE Transactions on Industry Applications*, vol. 49, no. 2, pp. 860–865, 2013.

[9] T. Roinila, H. Abdollahi, and E. Santi, "Frequency-domain identification based on pseudorandom sequences in analysis and control of dc power distribution systems: A review," *IEEE Transactions on Power Electronics*, vol. 36, no. 4, pp. 3744–3756, 2021.

[10] T. Roinila, M. Vilkko, and J. Sun, "Broadband methods for online grid impedance measurement," in *2013 IEEE Energy Conversion Congress and Exposition*. IEEE, 2013, pp. 3003–3010.

[11] A. Barkley and E. Santi, "Online monitoring of network impedances using digital network analyzer techniques," in *2009 Twenty-Fourth Annual IEEE Applied Power Electronics Conference and Exposition*. IEEE, 2009, pp. 440–446.

[12] A. Riccobono, M. Cupelli, A. Monti, E. Santi, T. Roinila, H. Abdollahi, S. Arrua, and R. A. Dougal, "Stability of shipboard dc power distribution: Online impedance-based systems methods," *IEEE Electrification Magazine*, vol. 5, no. 3, pp. 55–67, 2017.

[13] J. Siegers, E. Santi, and A. Barkley, "Wide bandwidth system identification of mvdc distribution system by applying perturbations to an existing converter," in *2013 IEEE Electric Ship Technologies Symposium (ESTS)*. IEEE, 2013, pp. 434–441.

[14] E. Liegmann, A. Riccobono, and A. Monti, "Wideband identification of impedance to improve accuracy and stability of power-hardware-in-the-loop simulations," in *2016 IEEE International Workshop on Applied Measurements for Power Systems (AMPS)*. IEEE, 2016, pp. 1–6.

[15] J. Ke, Z. Zhengxuan, Z. Qijuan, Y. Zhe, and B. Tianshu, "Islanding detection method of multi-port photovoltaic dc micro grid based on harmonic impedance measurement," *IET Renewable Power Generation*, vol. 13, no. 14, pp. 2604–2611, 2019. [Online]. Available: https://ietresearch.onlinelibrary.wiley.com/doi/abs/10.1049/iet-rpg.2019.0271

[16] R. W. A. A. De Doncker, D. M. Divan, and M. H. Kheraluwala, "A three-phase soft-switched high power density dc/dc converter for high power applications," in *Conference Record of the 1988 IEEE Industry Applications Society Annual Meeting*, 1988, pp. 796–805 vol.1.

[17] S. P. Engel, N. Soltau, H. Stagge, and R. W. de Doncker, "Dynamic and balanced control of three-phase high-power dual-active bridge dc–dc converters in dc-grid applications," *IEEE Transactions on Power Electronics*, vol. 28, no. 4, pp. 1880–1889, 2013.

[18] J. Hu, "Modulation and dynamic control of intelligent dual-active-bridge converter based substations for flexible dc grids," Ph.D. dissertation, RWTH Aachen University, Aachen, 2019.

[19] A. Riccobono, "Stabilizing controller design for a dc power distribution system using a passivity-based stability criterion," Ph.D. dissertation, University of South Carolina, 2013.

[20] R. Mencher, J. Mathé, and R. W. de Doncker, "Breaker-less mvdc-grid with single-phase dual-active bridge," in *2024 IEEE 10th International Power Electronics and Motion Control Conference (IPEMC2024-ECCE Asia)*. IEEE, 2024, pp. 979–983.

[21] S. P. Engel, N. Soltau, H. Stagge, and R. W. de Doncker, "Improved instantaneous current control for high-power three-phase dual-active bridge dc–dc converters," *IEEE Transactions on Power Electronics*, vol. 29, no. 8, pp. 4067–4077, 2014.